Rethinking the longitudinal stream temperature paradigm: region-wide comparison of thermal infrared imagery reveals unexpected complexity of river temperatures

Aimee H. Fullerton[1,2], Christian E. Torgersen[3], Joshua J. Lawler[2], Russell N. Faux[4], E. Ashley Steel[5], Timothy J. Beechie[1], Joseph L. Ebersole[6], and Scott G. Leibowitz[6]

[1] Fish Ecology Division, Northwest Fisheries Science Center, National Marine Fisheries Service, NOAA, 2725 Montlake Blvd E, Seattle, WA, 98112, USA; aimee.fullerton@noaa.gov

[2] School of Environmental and Forest Sciences, University of Washington, Seattle, WA, USA

[3] U.S. Geological Survey, Forest and Rangeland Ecosystem Science Center, Cascadia Field Station, University of Washington, Seattle, WA, USA

[4] Quantum Spatial, Inc., Corvallis, OR, USA

[5] Pacific Northwest Research Station, USDA Forest Service, Seattle, WA, USA

[6] National Health and Environmental Effects Research Laboratory, Western Ecology Division, U.S. Environmental Protection Agency, Corvallis, OR, USA

Keywords

Water temperature; remote sensing; longitudinal profile, spatial pattern

Key Points

- Many longitudinal river temperature patterns do not fit theoretical expectations
- Longitudinal patterns are diverse in shape and have no clear geographic trends
- Correlations with common predictors of water temperature vary among rivers

This article has been accepted for publication and undergone full peer review but has not been through the copyediting, typesetting, pagination and proofreading process, which may lead to differences between this version and the Version of Record. Please cite this article as doi: 10.1002/hyp.10506

Abstract

Prevailing theory suggests that stream temperature warms asymptotically in a downstream direction, beginning at the temperature of the source in the headwaters and leveling off downstream as it converges to match meteorological conditions. However, there have been few empirical examples of longitudinal patterns of temperature in large rivers due to a paucity of data. We constructed longitudinal thermal profiles (temperature versus distance) for 53 rivers in the Pacific Northwest (USA) using an extensive dataset of remotely sensed summertime river temperatures and classified each profile into one of five patterns of downstream warming: *asymptotic* (increasing then flattening), *linear* (increasing steadily), *uniform* (not changing), *parabolic* (increasing then decreasing), or *complex* (not fitting other classes). We evaluated (1) how frequently profiles warmed asymptotically downstream as expected, and (2) whether relationships between river temperature and common hydroclimatic variables differed by profile class. We found considerable diversity in profile shape, with 47% of rivers warming asymptotically, and 53% having alternative profile shapes. Water temperature did not warm substantially over the course of the river for coastal *parabolic* and *uniform* profiles, and for some *linear* and *complex* profiles. Profile classes showed no clear geographical trends. The degree of correlation between river temperature and hydroclimatic variables differed among profile classes, but there was overlap among classes. Water temperature in rivers with *asymptotic* or *parabolic* profiles was positively correlated with August air temperature, tributary temperature and velocity, and negatively correlated with elevation, August precipitation, gradient, and distance upstream. Conversely, associations were less apparent in rivers with *linear*, *uniform*, or *complex* profiles. Factors contributing to the unique shape of *parabolic* profiles differed for coastal and inland rivers, where downstream cooling was influenced locally by climate or cool water inputs, respectively. Potential drivers of shape for *complex* profiles were specific to each river. These thermal patterns indicate diverse thermal habitats that may promote resilience of aquatic biota to climate change. Without this spatial context, climate change models may incorrectly estimate loss of thermally suitable habitat.

Introduction

Temperature drives vital rates in aquatic biota and is a key determinant of ecological processes that control population and community structure in aquatic ecosystems (Allan and Castillo, 2007; Webb *et al.*, 2008). Substantial effort has focused on understanding temporal patterns in water temperature across hours, days, months, and years (Webb and Nobilis, 1995; Steel and Lange, 2007; Arismendi *et al.*, 2013), and recent research has underscored the biological significance of altered timing in riverine thermal regimes (Crozier *et al.*, 2008; Isaak *et al.*, 2012; Steel *et al.*, 2012). Spatial patterns in water temperature are also paramount to aquatic biota. For example, water temperature partly defines species distributions within and across river basins (Arscott *et al.*, 2001; Buisson *et al.*, 2008). At finer spatial scales (e.g., reaches of 1-10 km), water temperature can influence connectivity between reaches used during different life stages such as foraging and breeding (Tonolla *et al.*, 2010; Armstrong *et al.*, 2013).

There has been little evaluation of longitudinal spatial patterns in water temperature in large rivers. Therefore our understanding of thermal profiles and potential drivers remains incomplete. Prevailing theory dictates that stream temperature warms asymptotically in a downstream direction, beginning at the temperature of the source (e.g., groundwater or snowmelt) in the headwaters and leveling off downstream as it converges to an equilibrium determined by meteorological conditions (Vannote *et al.*, 1980; Theurer *et al.*, 1985; Ward, 1985; Bogan *et al.*, 2003). In downstream reaches, higher water volume increases thermal inertia, reducing the likelihood of rapid change in water temperature. It is now widely recognized that temperature can exhibit a high degree of variability between headwaters and the mouth (Poole and Berman, 2001; Poole, 2002; Brown and Hannah, 2008). However, the literature reveals that asymptotic warming is still generally the operating conceptual paradigm for longitudinal stream temperature patterns (Caissie, 2006; but see Dent *et al.*, 2008). Increasingly, large datasets are available that include water temperature compiled from point locations in many tributaries throughout and across watersheds (e.g., Isaak *et al.*, 2013). These data should improve our understanding about spatial patterns of water temperature, especially in wadeable streams where most empirical data are collected. Nevertheless, the degree of thermal complexity within and across large rivers remains unknown. Moreover, there have been few empirical studies examining the factors that drive these patterns (Deitchman and Loheide, 2012; Monk *et al.*, 2013; Dugdale *et al.*, 2015). Conceivably, climate is the dominant driver of temperature in some rivers, whereas landscape features such as terrain, geomorphology, and vegetation are more important in others.

Evaluation of these concepts will directly influence our understanding of anthropogenic impacts such as climate change on spatial patterns in river temperature.

In this paper, we use spatially continuous water temperature data from remote sensing to explore longitudinal patterns in synoptic summertime water temperature for 53 rivers throughout the Pacific Northwest (USA). Our objectives were to (1) classify river temperature profiles based on their shape and determine what proportion of profiles conform to the theoretical expectation of asymptotic downstream warming, and (2) evaluate whether relationships between river temperature and hydroclimatic variables differ by profile class. This work provides a spatial context for understanding long-term stream temperature predictions, which are instrumental to conservation planning.

Methods

Study Area

We considered a sample of watersheds across Washington, Oregon, Idaho, and northern California (USA). Precipitation in the region occurs predominantly from October to March and falls as snow or rain, depending mainly on elevation and proximity to the Pacific Ocean. Snowmelt contributes significantly to stream flow from April to September in snowmelt-dominated and transitional watersheds (Hamlet, 2010). Human population density in the study watersheds ranges from low (e.g., roadless areas in Idaho) to high (e.g., near major cities). Human influences on processes controlling hydrology and temperature include large hydropower facilities, water diversion for irrigation, forest management, and altered riparian vegetation associated with agriculture and urban development.

Water Temperature Data

River temperature surveys were conducted using airborne thermal infrared (TIR) remote sensing (Torgersen *et al.*, 2001; Madej *et al.*, 2006; Handcock *et al.*, 2012; Monk *et al.*, 2013). Thermal images measuring radiant temperature of surface water were acquired while flying directly over the river. The majority of surveys were conducted by Watershed Sciences Inc., Corvallis, OR (USA), using the approach described in Torgersen et al. (2001) and Monk et al. (2013). Different TIR sensors were used depending on the technology available at the time of the survey, but the sensor systems had comparable performance characteristics. All were similar in terms of wavelength range (8-12μm), radiometric calibration, and sensitivity. Earlier surveys (before 2001) used scanned arrays whereas later

surveys (2001 and after) used focal plane array sensors. Surveys in the Salmon and Clearwater rivers in Idaho were conducted by IRZ Consulting, Hermiston, OR (USA), using similar methods and a focal plane array sensor (ID DEQ 2000, 2001). All surveys occurred during the afternoon in July or August between 1994 and 2007, when water temperatures were expected to be near the daily and annual maximum and likely to be most limiting to aquatic biota (see Table 1 for specific dates). Instream thermal sensors were used to ground-truth remotely sensed temperatures; mean (± standard deviation) accuracy was 0.44 ± 0.37 °C (Table 1). Thermal image data were georeferenced and water temperatures were subsampled from images at approximately 150- to 200-m intervals along the thalweg of each river. We created longitudinal profiles for each river using plots of water temperature versus distance from the downstream end of the survey.

To maximize the extent of river available for characterizing the longitudinal thermal profile from headwaters to mouth, we combined adjacent surveys to construct profiles. For 14 profiles, we combined adjacent surveys conducted on the same day (see Table A1). Separate surveys in upstream and downstream sections were flown continuously (i.e., without stopping) on the same day for 8 profiles. For the remaining 6 profiles, surveys were separated by ≤1 h (5 surveys) and 2.5 h (1 survey). Differences in water temperature at the junction between upstream and downstream sections were only visible for 2 of 14 profiles and both of these discrepancies were attributable to tributary confluence effects. For another 14 profiles, we combined adjacent surveys that were flown at similar times but on separate days (see Table A2). Weather conditions were alike on days during which combined surveys occurred. Seven of these profiles exhibited differences in water temperature at the junctions between surveys; these differences were due to tributary confluences in 5 cases. Two profiles had unexplained discrepancies at junctions between surveys but these differences did not influence our interpretation of the shapes of the profiles.

Flight duration and direction may influence the interpretation of the shape of longitudinal thermal profiles because daily maximums are typically reached earlier in upstream reaches (downstream reaches warm more slowly due to thermal inertia of larger volumes). For example, Torgersen *et al.* (2001) found that temperatures increased at a maximum rate of about 1°C h^{-1} in upper reaches and at slower rates in lower reaches. Therefore, the potential for misclassification increases with survey duration. In our study, combined flight time averaged 1.6 h for profiles constructed from surveys conducted on the same day and 3.0 h for surveys conducted on separate days. The combined flight time for profiles constructed from multi-day surveys tended to be longer overall, but surveys were

conducted during the same window of time each day; individual surveys on a given day averaged 1.45 h. Changes in water temperature over the course of each survey measured with instream sensors were typically 0.5 °C but were as high as 2 °C in one survey. Although most surveys proceeded in an upstream direction, 14 profiles were flown at least partly in a downstream direction; 9 of these profiles were combined surveys (Table 1). If flight direction biased our interpretation of longitudinal profile shapes (see Table A3), it was in the same direction for most surveys. Bias is likely to be greatest for profiles surveyed in a downstream direction and in small rivers. Our profiles that were surveyed in a downstream direction occurred in rivers with a mean stream order of 4.8 ± 0.9; the longitudinal thermal profiles for two rivers with stream orders <4 had strong shapes unlikely to have been influenced by flight direction.

To be included in our analysis, a profile dataset had to meet the following criteria: (1) total surveyed length of the river was at least 50 km; (2) surveyed length was no less than 50% of total river length, measured from the mouth (the ocean or confluence with a larger river) to the top of the uppermost second-order reach in a 1:100,000-scale digitized stream network (NHDPlusV2; McKay *et al.*, 2012); (3) the profile spanned at least two Strahler stream orders; and (4) the midpoint of the profile was located within the middle one-third of the river. These criteria ensured that we had sufficient longitudinal data to describe temperature profiles and to make comparisons among rivers. Using these criteria, we retained 58 profiles in 53 rivers from an initial population of nearly 500 surveys (see Figure A1).

Surveys were conducted twice over approximately the same extent in 4 rivers: the Applegate (1998, 1999), Middle Fork John Day (1998, 2003), Sprague (1999, 2007) and Walla Walla (2000, 2003). Surveys covered overlapping but different reaches in the Scott River (2003, 2006). Longitudinal profiles from repeat surveys demonstrate consistent spatial patterns among years (Figure 1).

Contemporaneous discharge data was available for 44 profiles and enabled us to identify profiles that may have been influenced by unusual flow conditions (Table 1) or by dams (Table 2). For each of these profiles, we used data from all USGS gages located within the same spatial extent covered by TIR surveys to compute the average discharge for the month and year in which the TIR survey occurred. We then compared this value to the monthly average (for the same month) from gage data over the period of record for that location. We also evaluated the influence of our selection criteria on our conclusions by examining whether the relative proportion of rivers in each profile class differed when we relaxed the criteria (see Table A4 for descriptions of additional profiles that were considered).

Statistical Analyses

Preliminary inspection of thermal profiles suggested five classes of longitudinal pattern (described below, plots and equations in Figure 2). We hypothesized geographic locations where each pattern was likely to occur and the factors that may drive its configuration. We then evaluated the proportion of empirical profiles that fit these classes, examined their geographic distribution, and compared relationships between river temperature and hydroclimatic and network variables for rivers in each profile class. The five profile classes and their hypothesized characteristics are listed below:

Asymptotic: nonlinear warming from headwaters to the mouth in a saturating pattern. Originates at high elevations and moves downstream into arid flatlands where water is exposed to solar radiation with few opportunities for cooling by riparian shading or groundwater. We hypothesized that this type is likely to occur in areas of the Columbia Plateau (Theurer *et al.*, 1985; Ward, 1985; Caissie, 2006; Allen, 2008).

Linear: constant warming from headwaters to the mouth. Originates at high elevations and progresses downstream over steep slopes with few discontinuities in the heat budget (e.g., having numerous small but few large groundwater or tributary inputs, and gradual changes in riparian vegetation). We hypothesized that this type would be likely to occur on the slopes of mountain ranges such as the western Cascade Range in Oregon (USA) (Torgersen *et al.*, 1999; Tague *et al.*, 2007; Tague *et al.*, 2008).

Parabolic: rapid warming from headwaters to a maximum, and then cooling again downstream. Originates at high elevations, transitions through wide alluvial valleys with increased exposure to solar radiation, then flows through a zone of cooling downstream. Cooling may be caused by local climate (e.g., coastal fog), influx of groundwater, impermeable geology and steep topography, or a combination of the above factors. Examples found along the Pacific coast (Madej *et al.*, 2006).

Uniform: temperature remains constant with distance. Streams flow through relatively homogenous terrain (i.e., with similar geology and little change in elevation) with shading or groundwater inputs that prevent warming. We hypothesized that this type was likely to occur in flat portions of the Interior Columbia basin (Allan and Castillo, 2007).

Complex: profiles with multiple discontinuities (increasing and/or decreasing). Discontinuities may be caused by stream topology (i.e., position and layout of tributaries in the stream network), geomorphology, interaction with groundwater, or other local

controls (natural or anthropogenic, such as the presence of dams). We hypothesized that this type would be likely to occur in topographically complex areas (Oregon Department of Environmental Quality *et al.*, 2001; Kiffney *et al.*, 2006).

Model Selection

We classified each empirical profile as *asymptotic*, *linear*, *parabolic*, or *uniform*. If none of these models was appropriate, the profile was considered *complex*.

We used generalized least squares regression (Pinheiro and Bates, 2000) to fit each of four model forms to each river temperature profile (see Figure 2 for equations). Water temperatures within a river were always highly spatially autocorrelated ($\Phi \sim 0.8$ to 0.99), with temperature at one location being dependent on temperature just upstream. Inspection of autocorrelation and partial autocorrelation functions suggested that a first-order autoregressive error process was appropriate, so we included this error structure when fitting models. Analyses were conducted in R (R Development Core Team, 2012) using the *gls* and *gnls* functions with a *corAR1* error structure (Pinheiro *et al.*, 2012). We used the following constraints when fitting each model: (1) a *linear* model had a negative slope, cooler in headwaters than near the mouth ($m<0$); (2) a *parabolic* model was convex with a maximum not located at the river mouth ($a<0$, $b>0$); (3) an *asymptotic* model increased rapidly near the headwaters and then gradually toward the mouth ($a<0$, $m>0$); (4) a *uniform* model was an intercept-only model with a slope of 0. If the conditions for a thermal profile were violated, that model was discarded from that profile's candidate set. The best model among the remaining candidate models was the one having the greatest Akaike weight (Burnham and Anderson, 2002). To be conservative, we chose *parabolic* only when its ΔAIC was >10 units better than any other model, which placed a greater burden of proof on finding this unusual pattern.

We evaluated whether the best model fit the data using four metrics: (1) root mean squared error (RMSE; Eq. 1), (2) the Nash-Sutcliffe model efficiency coefficient (NSC; Nash and Sutcliffe, 1970; Eq. 2), (3) p-values from a Glejser test (Glejser, 1969) for heteroscedasticity, and (4) the difference between RMSE for the best model and RMSE for a smoothed (20-knot GAM) model. The fourth metric represented spatial structure not captured by the trend in the best model. The first two metrics were computed respectively as:

$$RMSE = \sqrt{\frac{1}{N}\sum_{i=1}^{N}(F_i - O_i)^2} \quad \text{[Eq. 1]}$$

$$NSC = 1 - \frac{\sum_{i=1}^{N}(F_i - O_i)^2}{\sum_{i=1}^{N}(O_i - \bar{O})^2} \quad \text{[Eq. 2]}$$

where O_i is observed temperature at point i of the survey, F_i is fitted temperature from the best model, and N is the number of observations along the length of the profile.

We used a point system to decide whether to classify a profile as *complex*. We assigned points ranging from 1 (a good fit) to 4 (a poor fit) to each of the 4 metrics. Scores corresponded to quartiles for each metric computed across the set of profiles. We summed the 4 scores to get a total score ranging between 4 and 16. Profiles having scores of 10 or lower (i.e., having adequate fits) retained their classification as *asymptotic*, *linear*, *parabolic*, or *uniform*, while those having scores of 14 or more (i.e., failing most diagnostics) were classified as *complex*. Profiles with scores between 11 and 13 and profiles with scores <11 but having ΔAIC <2 better than the second best model retained their original classification, but we highlighted them as profiles for which classification was less certain. We inspected four types of diagnostic plots to evaluate the scores: (1) observed versus expected values, (2) residuals from the best model, (3) residuals from the smoothed model, and (4) fitted values from a 5-knot GAM compared to those from the best model.

Additionally, we compared profile shapes selected quantitatively (as described above) with qualitative visual assignments. Four of the authors (not including the lead author) each assigned a shape, a level of confidence in their assessment, and potential alternative shapes to each profile; this was a blind process, i.e., authors did not know the names of the rivers they were assessing. We used the majority class from the qualitative assessments for each profile to evaluate robustness of the quantitative classification.

Associations with Hydroclimatic and Network Variables

We evaluated whether relationships between river temperature and hydroclimatic variables (described below) differed among profile classes. For each thermal profile, we evaluated correlations between water temperature and hydroclimatic variables discretized at 1-km intervals along the length of the profile after accounting for spatial autocorrelation. First, we binned mean values of both river temperature and hydroclimatic variables (described below) at 1-km intervals to ensure that water temperature and hydroclimatic

variables were spatially matched at the same resolution along the length of each river (Welty *et al.*, 2015). Then, for each profile, we computed the partial correlation coefficient between water temperature and each hydroclimatic variable. Partial correlation coefficients were computed as the correlation between (1) the residuals of a linear model between river temperature and distance upstream and (2) the residuals of a linear model between a given hydroclimatic variable and distance upstream. The goal of this approach was to examine relationships between river temperature and hydroclimatic variables after we had accounted for their mutual correlation with space (Legendre, 1993). We also computed the correlation coefficient between river temperature and distance upstream.

We considered variables that are frequently used in predictive models of water temperature and in response to climate change impacts: mean August air temperature (°C), mean August precipitation (mm), elevation (m), discharge (m^3s^{-1}), velocity (ms^{-1}), stream gradient (%), and water temperature in tributaries. Data for the first 6 explanatory variables came from attributes of 1:100,000-scale stream reaches in NHDPlusV2 (McKay *et al.*, 2012), which is a geospatial framework of surface-water data products based partly on the U.S. National Hydrography Dataset (see Table A5). The NHDPlusV2 is a GIS dataset comprising estimates of elevation, gradient, air temperature, precipitation, discharge and stream velocity for all reaches within rivers of the United States. Elevation, gradient and velocity were derived from a 10-m digital elevation model. Air temperature and precipitation estimates were derived from the PRISM model (www.prismclimate.org). Discharge and velocity were calculated using the enhanced runoff method (EROM), and values were adjusted to gages at the bottom of each reach (McKay *et al.*, 2012). Tributary temperatures were sampled at the confluence of the tributary with the main river from TIR imagery.

We used partial correlation coefficients as inputs to a principal components analysis (PCA) to visualize groups of profile classes in relation to hydroclimatic variables. Using partial correlation coefficients in the PCA, as opposed to aggregate metrics summarized across all reaches in a profile, allowed us to examine the spatial relationship between hydroclimatic variables and river temperature over the profile length. We expected that profiles of the same class would be clustered in the PCA if river temperature was spatially correlated with the same suite of hydroclimatic variables as other profiles in that class.

We also evaluated relationships between profile classes and 3 network variables: (1) significant confluence density, where significant confluences were defined as tributary confluences contributing more than 10% of mainstem flow, (2) stream density, or length of streams per catchment area, and (3) basin shape, defined as the drainage area divided by the

square of the mainstem length. We anticipated that *complex* thermal profiles would be associated with streams having larger values of significant confluence density, stream density and basin shape (Benda *et al.*, 2004).

Results

Profile Classification

We classified 27 longitudinal thermal profiles as *asymptotic*, 9 as *linear*, 8 as *parabolic*, 4 as *uniform*, and 10 as *complex* (Figure 3; also see Figure A2). For 25 thermal profiles, classification was not definitive (Table 3). In 2 of these cases, the *asymptotic* model did not converge. For these rivers (John Day and NF John Day), the fit of the next best model (*linear*) was relatively poor (goodness of fit scores of 16 and 12, respectively), so we used the qualitative assignment of *asymptotic* assessed visually by the coauthors. In three other cases (Grande Ronde River, Whychus Creek and Williamson River), the best models selected were *linear*, *linear* and *uniform*, respectively. However, we assigned these profiles as *complex* because quantitative fits were relatively poor (goodness of fit scores of 13, 12, and 11 points, respectively, and ΔAIC of <1 between best and second best models). Moreover, qualitative assessments by the coauthors were unanimous in classifying these profiles as *complex*. We list the best and second choices in Table 1. For profiles classified as *complex*, we list the best quantitative assignment as the second choice. Distributions of profiles among classes based on the second choice were similar to 'best' choices; the most notable difference was that there were more *linear* and *complex* profiles and fewer profiles in the other classes (see Table A6). The shapes of the profiles were consistent from year to year for rivers that had been surveyed multiple times: Applegate, Middle Fork John Day, Sprague, and Walla Walla rivers (Figure 1; Table 1).

Qualitative assessments were consistent with the quantitative approach for 41 profiles (71%). Disagreement between the qualitative and quantitative approaches occurred among all five classes. Using the majority class visually assessed by 4 coauthors, profiles assigned as *asymptotic* by the quantitative method were described as *linear* (5 cases), *uniform* (2 cases), or *complex* (2 cases) by the visual assessments; *linear* profiles were described as *uniform* (1 case) or *complex* (2 cases) by the visual assessments; 1 *uniform* profile was described as *complex*; and 1 *complex* profile was described as *asymptotic* by the visual assessments. For profiles classified as *parabolic* by the quantitative approach, 4 were classified as *asymptotic* by visual assessments: Eightmile Creek, Fifteenmile Creek, and Walla Walla River in both

2000 and 2003. These 3 rivers are inland tributaries to the Columbia River, whereas the other 4, upon which both qualitative and quantitative classification agreed were truly *parabolic* shapes, flowed directly to the Pacific Ocean. We treated these cases separately in subsequent analyses and address these points in the discussion.

Contrary to our expectations, the spatial distribution of profile classes did not suggest any clear geographical patterns (Figure 4). One exception is that the 4 profiles classified as *parabolic* by both quantitative and qualitative methods were located on the Pacific coast.

Influence of Discharge, Dams, and Flight Direction

Profile shape may have been influenced by flow conditions during the survey year (Table 1). In 10 cases, rivers were surveyed during years in which discharge was substantially higher than average (i.e., above the 75th percentile over the period of record for that location); 8 surveys occurred during low-discharge years (i.e., below the 25th percentile). However, the distribution of profile shapes was similar for high and low flow years, with 6 and 5 *asymptotic*, 4 and 3 *linear*, 1 and 0 *parabolic*, 0 and 1 *uniform*, and 1 and 0 *complex*, respectively. Conditions differed between years for repeat surveys in the Middle Fork John Day and Sprague rivers; discharge was high in only the first year for the former and low in only the second year for the latter. Discharge was high in both years for the Applegate River, and normal in both years for the Walla Walla River. Profile classification was consistent between years for all repeat surveys.

Our ability to distinguish profile shape may also have been influenced by dams (Table 2). It is possible that dams located in the upper reaches of surveys (5 cases) may have influenced upstream thermal conditions (sensu Ward and Stanford, 1983). However, it is unlikely that the *asymptotic* shape of the Rogue River would change in the absence of the dam because there was a strong downstream warming trend for >150 km. The Applegate River, Cow Creek, and Russian River also likely would remain *asymptotic* in the absence of a dam upstream; however, downstream warming trends were less pronounced in these rivers so it is possible that their profiles would be *linear* if the effect of the dams was to cool the upper reaches of the profile (i.e., downstream from dams). The Shasta River, classified as *linear*, could possibly be *asymptotic* if the effect of the dam was to moderate temperatures in upper reaches. Two of the profiles classified as complex showed potential dam influences in the middle of the profile. The large decrease in water temperature in a downstream direction in the Tualatin River was due to inputs of cold water from Scoggins Creek, which originated as bottom releases from Scoggins Dam. The Tualatin River profile may otherwise have been

asymptotic or *linear*. The Crooked River was also strongly influenced by Arthur R. Bowman Dam near Prineville, OR (USA), which lowered water temperatures substantially in the middle section of the longitudinal thermal profile. This river would have been classified as *complex* regardless of the dam, due to inputs of large volumes of cooler water via lava tubes and other subsurface pathways.

It is also possible that flight direction influenced classification. For rivers surveyed in an upstream direction, it is possible that true *asymptotic* profiles may have been classified as *linear* or *uniform* if headwaters warmed rapidly (see Table A3). Conversely, for rivers surveyed in a downstream direction, true *linear* or *uniform* profiles may have been misclassified as *asymptotic* if headwaters were surveyed before they reached their maximum temperature.

Inclusion Filter Criteria

The inclusion criteria that we applied to ensure that the profiles were representative of whole-river patterns were generally similar across profile classes (Table 3); these inclusion criteria were river length, proportion of river surveyed, survey midpoints, the number of stream orders spanned and the mean stream order. Profiles classified as *uniform* and *linear* tended to be slightly shorter, covered a smaller proportion of the river and fewer stream orders, and had midpoints downstream compared to other classes. Profiles classified as *parabolic* and *complex* were the longest, had the highest proportion of river surveyed and had the greatest range in stream order. *Asymptotic* profiles had intermediate values for most metrics. Coastal *parabolic* rivers had lower mean stream order than other types. Had we used relaxed criteria, we would have included an additional 10 profiles, with 3 included by removing the stream order criterion and 7 by relaxing the longitudinal position criterion (to allow midpoints centered between 25 and 75% of river length). With these additional profiles, the percent of profiles in each shape class remained within ~2% of original numbers (see Table A6).

Associations with Hydroclimatic and Network Variables

Hydroclimatic Variables

Correlations between river temperature and hydroclimatic variables differed among profile classes (Table 4). In particular, we noticed high variability across classes in the correlation between water temperature and August air temperature after accounting for correlation with distance upstream (Table A7). For rivers classified as *asymptotic* and for

inland *parabolic* rivers, water temperature was positively correlated with August air temperature, tributary temperature and velocity, and negatively correlated with elevation, August precipitation, gradient, and distance upstream (Table 4). Partial correlation coefficients for coastal *parabolic* profiles were smaller but in the same direction as coefficients for inland *parabolic* profiles for elevation, mean August Air temperature, mean August precipitation, gradient, and tributary temperature. Coastal profiles had a more negative coefficient for discharge, whereas inland profiles had a more negative coefficient for distance upstream. In contrast, for rivers classified as *linear*, *uniform*, or *complex*, partial correlation coefficients were small for most hydroclimatic variables. Water temperature for rivers with *linear* profiles was negatively correlated with distance upstream; this coefficient was larger than coefficients for hydroclimatic variables. Water temperature was more strongly correlated with tributary temperature for rivers with inland *parabolic*, *complex*, and *uniform* profiles than for other profile shapes. Water temperature was negatively correlated with distance upstream for *asymptotic*, *linear*, and inland *parabolic* profiles but poorly correlated for coastal *parabolic* rivers and rivers classified as *uniform* or *complex*.

Differences among profile classes in relationships between river temperature and hydroclimatic variables were visually apparent when we plotted the profiles on the same scale. For instance, after accounting for the shared correlation with distance upstream, water temperature was more positively correlated with August air temperature for *asymptotic* and *parabolic* profiles than for *linear*, *uniform*, or *complex* profiles (Figure 5). Figure 5 also illustrates that many profiles (e.g., coastal *parabolic*, *linear*, *uniform*, *complex*, and even some *asymptotic* profiles were relatively flat over their course. These patterns persisted when we included profiles that met a relaxed set of criteria.

The different profile classes fell into relatively distinct but overlapping domains in multivariate space (Figure 6). The first and second principal components of the PCA accounted for about 36 and 19% of the variance, respectively; only the first two axes were significant ($p<0.001$). Profiles in the *uniform* and *linear* classes were most different from the *asymptotic* class along the first axis (PC1); this pattern was evident primarily in the strength of correlations between river temperature and climate variables. Profiles in the *linear* and *asymptotic* classes were most different from the *uniform* and *parabolic* profiles along the second axis (PC2), which indicates gradients in hydrologic variables and distance upstream. The position of rivers in the *parabolic* class depended on regional location. Inland *parabolic* profiles (4 surveys in 3 rivers) overlapped with *asymptotic* profiles, whereas coastal *parabolic* profiles (4 rivers) were intermediate between *asymptotic* and *uniform* classes.

Profiles in the *complex* class overlapped with other classes in ordination space, which is consistent with the observed high variance in correlations between water temperature and most variables for *complex* profiles.

Network Variables

We did not detect any strong associations between profile classes and network variables (i.e., there was high within-class variability; Table 5), but profiles that did not exhibit warming in a downstream direction (e.g., coastal *parabolic* and *uniform*) tended to have a higher density of significant confluences. Contrary to expectations, *complex* profiles had the lowest stream density and also had moderate values for the density of significant confluences and basin shape. Coastal *parabolic* profiles were the least compact in shape (i.e., more likely to be rectangular than heart or pear shaped; sensu Benda *et al*. 2004), which is consistent with their generally lower stream order.

Discussion

Rethinking the Downstream Warming Paradigm

River scientists have recognized that the conceptual model of asymptotic stream warming from headwaters to mouth may not apply in all rivers (Moore *et al.*, 2005; Brown and Hannah, 2008; Dent *et al.*, 2008). However, the high-resolution spatial data needed to evaluate longitudinal profile patterns in and across large rivers has been lacking until now. Using an extensive, detailed dataset of spatially continuous summertime river temperatures, we found that water temperature did not always warm asymptotically in a downstream direction, as expected. Rather, we found evidence of at least four other profile shapes. Although *complex* and *linear* shapes were expected based on the literature, the *uniform* and *parabolic* shapes were unexpected. Our intent was not to promote our particular profile classification scheme *per se*; rather, we wanted to illustrate that there are rivers that exhibit alternative and sometimes unexpected longitudinal profile shapes. Matching profile classifications from repeat surveys of four rivers suggest that patterns were consistent among years, but additional data are needed to fully assess temporal stability of patterns.

Asymptotic downstream warming represents the foundation of a longitudinal stream temperature typology for many rivers. It is possible that some of the rivers that we classified as *linear* or *uniform* may represent adjacent parts of a larger asymptotic warming pattern if (1) these profile classes were shorter as a proportion of total river length than other classes,

(2) *linear* profiles occurred closer to headwaters than other classes, and (3) *uniform* profiles occurred closer to river mouths than other classes. In our analyses, both *linear* and *uniform* rivers were shorter on average and were shorter as a proportion of total river length than other classes (Table 3). Thus, it is possible that we misclassified some *asymptotic* rivers as (1) *uniform* because the surveys did not include colder headwater stream reaches, or (2) *linear* because the surveys did not extend far enough downstream to detect the asymptote. Rivers classified as *uniform* did tend to occur close to river mouths; however, rivers that were classified as *linear* also occurred near river mouths.

We expected that many rivers would exhibit downstream sections with little or no increases in temperature in a downstream direction based on the asymptotic conceptual model for downstream warming. However, rivers that we classified as *uniform* (e.g., Deschutes [Puget Sound] and Pudding rivers) were surveyed from the headwaters to the mouth. Furthermore, many of the rivers that we classified as *asymptotic* could have been classified as *linear* or *uniform* because their downstream inflection points were not very pronounced and their rates of warming were minimal (see Figure A2). In fact, many of the visual assessments did assign these rivers to *linear* or *uniform* classes (e.g., the Hoh River).

Parabolic or *complex* profile types may indicate an underlying asymptotic downstream warming pattern that is influenced by local factors that disrupt the expected downstream warming trend. We did not find any examples for either shape that could have been caused by surveying an incomplete portion of the river; *parabolic* and *complex* profiles covered 92% and 97% of total river length, respectively, and both shapes were centered within rivers (Table 3). These patterns were more common than we expected based on the literature. Moreover, we found other examples of rivers that fit alternative patterns of downstream warming when we examined longitudinal profiles of recently published modeled mean August (1993-2011) water temperature from the NorWeST project (Isaak *et al.*, 2013).

Our analysis focused on trends in river temperature at very broad spatial scales (>50 km), but more research is needed to examine longitudinal complexity in stream temperature at finer spatial scales using alternative metrics. For example, Dugdale *et al.* (2013) quantified thermal complexity in an Atlantic salmon river using the standard deviation of derivatives of the long profile calculated within a 1-km moving window, and Dent *et al.* (2008) quantified the length of reaches in coastal Oregon headwater streams that were decreasing, constant, or increasing in temperature. Spatially continuous river-temperature data, such as the TIR dataset used in this study, are becoming more available, as are spatially continuous modeled stream temperature maps that cover broad spatial extents (Isaak *et al.*, 2013; Peterson *et al.*,

2013; Isaak *et al.*, 2014). These datasets are powerful tools that will make it possible to better quantify complex thermal patterns in rivers.

Potential Drivers of Longitudinal Spatial Patterns

Spatial relationships between river temperature and hydroclimatic variables suggest that longitudinal thermal profile shapes are influenced by local and regional conditions. Rivers that originated at higher elevations with higher precipitation and flowed through arid regions tended to be cool in the headwaters and warm rapidly or steadily as the river progressed downstream. In these rivers, the headwaters may be cool due to a combination of snowmelt, relatively greater riparian shading than downstream, and steeper gradient (i.e., less time to equilibrate with air temperatures). These patterns were associated with *asymptotic*, *linear*, and inland *parabolic* profile types, which also had lower densities of significant confluences than other profile shapes (Table 5).

Water temperature in rivers that did not warm substantially in a downstream direction (i.e., *uniform*, *complex*, coastal *parabolic*, and some *linear* profiles) was less correlated with many of the hydroclimatic variables that we tested. For rivers exhibiting the *parabolic* pattern, there were at least two potential mechanisms controlling cooling near the mouth: local climate conditions and cold water inputs. In coastal rivers, reduced water temperature occurred in downstream reaches and may be influenced by fog cover (Madej *et al.*, 2006) (Figure 6). The cooling mechanism for these rivers may be reduced solar radiation reaching the river under heavy fog and an increased contribution of atmospheric moisture to the river (i.e., condensed and trapped in riparian areas; Harr, 1982). In contrast, inland rivers had air temperatures that were generally warmer near the river mouth, suggesting that cooling was more likely driven by inputs of cool water from tributaries, surficial aquifers (Arrigoni *et al.*, 2008; van Vliet *et al.*, 2013; Ebersole *et al.*, 2015), or other influences, such as shading from riparian vegetation or evaporative cooling from strong winds (Figure 6). The relatively constant temperatures in *uniform* and coastal *parabolic* rivers may be moderated by surficial or subsurface inputs of cooler water throughout, as evidenced by higher densities of streams and significant confluences. Rivers with *uniform* or coastal *parabolic* shapes also did not have large changes in elevation over the course of the river.

In rivers with *complex* profile shapes, and in many rivers with other shapes, abrupt changes in temperature were apparent at finer spatial scales that obscured broader patterns. Anomalies within thermal profiles may arise from local conditions that differ across the landscape (Ward and Stanford, 1983; Stanford and Ward, 2001; Poole, 2002). Discontinuities

in thermal profiles can be caused by tributaries (Rice *et al.*, 2001; Kiffney *et al.*, 2006; Ebersole *et al.*, 2015) or surface-groundwater exchange (Constantz, 1998; Keery *et al.*, 2007), which can contribute a substantial volume of water of a different temperature to the river. Discontinuities also may be due to localized shade produced by riparian vegetation (Beschta, 1997; Brosofske *et al.*, 1997) or to topographic characteristics such as aspect or valley confinement (Constantz, 1998; Poole, 2002). Tributaries and surface-groundwater exchange can decrease water temperatures directly via inputs of cooler water, whereas shade and topography prevent warming over a given distance by decreasing the duration that water is exposed to solar radiation. Moreover, factors contributing to discontinuities in the longitudinal thermal profile are likely to be different in different parts of the river. Poole and Berman (2001) suggested that riparian shading may be a more important determinant of locally cool conditions in headwaters, whereas surface (and subsurface) inputs may dominate in downstream reaches. Discontinuities also can be caused by human impacts. For example, dams can change downstream thermal conditions depending on how water is released from reservoirs (i.e., surface or bottom releases), as we saw for the Tualatin and Crooked rivers. The Crooked River also was influenced by high-volume subsurface inputs of cool water near the mouth via lava tubes and other subsurface pathways.

Associations between water temperature and hydroclimatic and network variables generally supported our hypotheses about potential drivers of longitudinal river temperature patterns. However, many of our hypotheses were incorrect about where the different types of profiles were likely to occur geographically. With the exception of coastal *parabolic* rivers being located along the Pacific coast, rivers with similar longitudinal profile shapes were not associated with specific physiographic regions and landscape features in the Pacific Northwest.

Implications for Ecology and Conservation

Our results have implications for biological conservation and management of riverine thermal regimes (Hamlet, 2010; Kaushal *et al.*, 2010; IPCC *et al.*, 2014), aquatic biota, and ecosystem processes (Ficke *et al.*, 2007; Mantua *et al.*, 2010), which respond to climate change and other anthropogenic impacts. First, our findings illustrate the variety of spatial patterns of summertime thermal habitat present within and among rivers. Cold-water organisms in rivers may be able to use thermal diversity in rivers to survive in a warming climate. Concepts from metapopulation biology (Hanski, 1998) and portfolio theory (Schindler *et al.*, 2010) suggest that diverse habitats may promote resilience to disturbance,

such as warmer water temperature. Although we did not investigate thermal patterns at finer spatial scales in this manuscript, the variability in spatial patterns in river temperature that we observed suggest the presence of potential cold-water refuges at multiple spatial scales. Such refuges are used by aquatic organisms in their movement among breeding, foraging and rearing habitats (Schlosser, 1995; Torgersen *et al.*, 1999; Dugdale *et al.*, 2013; Ebersole *et al.*, 2015).

An understanding of locations where local controls such as geomorphology, tributary influence, groundwater exchange points, and riparian vegetation may outweigh climate effects could provide a sense of a river's "natural" thermal regime (Hill *et al.*, 2013), its sensitivity to change (Luce *et al.*, 2014), and its potential for restoration (Ebersole *et al.*, 1997). Such information will be essential for prioritizing conservation actions that provide long-term benefits. Spatially continuous data on stream temperature from remote sensing and modeling provide a context for understanding longitudinal thermal profiles and establishing total maximum daily load (TMDL) thermal requirements to enhance water quality in rivers.

Models predicting the response of water temperature to climate change will need to consider spatial patterns of water temperature and the drivers of riverine thermal regimes. Existing models that assess climate-change effects on river temperatures at broad scales (i.e., large in extent and coarse in resolution) have generally predicted that future river temperatures will exhibit a pattern of asymptotic warming from headwaters to mouth (e.g., Allen, 2008) and that water temperature will respond similarly across space to changes in air temperature and stream flow (van Vliet *et al.*, 2011; Mayer, 2012; Wu *et al.*, 2012). Our study found that existing river temperature profiles are complex and variable with respect to basic climate variables, suggesting that climate change may affect river temperature differently among rivers.

Conclusions

Until recently, data to characterize spatial patterns in river temperature over broad spatial extents were unavailable. In our analysis of remotely sensed water temperature data, we did not expect to find that many rivers throughout the Pacific Northwest (USA) did not warm asymptotically in a downstream direction. Instead, more than half of the rivers we evaluated exhibited one of several unusual longitudinal profile patterns, and many rivers were too complex to classify with a simple model. Moreover, relationships between water temperature and basic hydroclimatic variables differed among profile classes. Our approach and results may serve as a starting point for classifying longitudinal thermal profiles and

assessing potential human impacts on stream temperature patterns at scales of tens of kilometers. Without this spatial context, climate impacts to thermal habitat may be difficult to predict because longitudinal patterns are influenced by myriad local and regional controls that may respond differently to changes in climate.

Acknowledgments

Individual river temperature surveys and image processing were conducted by R. Faux, Watershed Sciences Inc., except for rivers in the Salmon and Clearwater basins in Idaho, the data for which were provided by D. Essig of the Idaho Department of Environmental Quality. We are grateful to the many local, state, federal, tribal and nongovernmental organizations that funded the collection of these data for water quality monitoring and assessment. AHF was supported by the Northwest Fisheries Science Center and the NOAA Advanced Studies Program. We thank P.M. Kiffney, N.J. Mantua, S.G. Smith and three anonymous reviewers for helpful discussions and reviews of earlier versions of the manuscript, and B.J. Burke for statistical advice. The information in this document has been subjected to peer and administrative review and is approved for publication by NOAA, USGS, EPA, and USFS. Any use of trade, product, or firm names is for descriptive purposes only and does not imply endorsement by the U.S. government.

Supplementary Information

Table A1. Data specifications for combined adjacent surveys conducted on the same day

Table A2. Data specifications for combined adjacent surveys conducted on different days

Table A3. Potential implications of flight direction on profile classification

Table A4. Attributes of remotely sensed profiles of summertime river temperature that met relaxed filter criteria and which were used only in supplementary analyses

Table A5. Hydroclimatic variables summarized over all reaches in each profile of remotely sensed summertime water temperature

Table A6. The number and percent of longitudinal profiles belonging to each profile class under strict versus relaxed inclusion criteria, and comparing first and second best profile classes

Table A7. Hydroclimatic and network variables associated with each profile

Figure A1. Map of the spatial extents of thermal infrared surveys used to evaluate shapes of thermal profiles

Figure A2. Longitudinal profiles of river temperature (°C) versus distance upstream (km) for each river that met strict criteria for inclusion in analyses

References

Allan JD, Castillo MM. 2007. *Stream Ecology: Structure and Function of Running Waters, 2nd edition.*, Springer.

Allen DM. 2008. Development and application of a process-based, basin-scale stream temperature model. PhD Thesis. University of California, Berkely, CA.

Arismendi I, Johnson SL, Dunham JB, Haggerty R. 2013. Descriptors of natural thermal regimes in streams and their responsiveness to change in the Pacific Northwest of North America. Freshwater Biol, **58**: 880-894. DOI: 10.1111/Fwb.12094.

Armstrong JB, Schindler DE, Ruff CP, Brooks GT, Bentley KE, Torgersen CE. 2013. Diel horizontal migration in streams: juvenile fish exploit spatial heterogeneity in thermal and trophic resources. Ecology, **94**: 2066–2075. DOI: 10.1890/12-1200.1.

Arrigoni AS, Poole GC, Mertes LAK, O'Daniel SJ, Woessner WW, Thomas SA. 2008. Buffered, lagged, or cooled? Disentangling hyporheic influences on temperature cycles in stream channels. Wat. Res. Research, **44**: n/a-n/a. DOI: 10.1029/2007wr006480.

Arscott DB, Tockner K, Ward JV. 2001. Thermal heterogeneity along a braided floodplain river (Tagliamento River, northeastern Italy). Can J Fish Aquat Sci, **58**: 2359-2373. DOI: 10.1139/cjfas-58-12-2359.

Benda L, Poff NL, Miller D, Dunne T, Reeves G, Pess G, Pollock M. 2004. The network dynamics hypothesis: How channel networks structure riverine habitats. Bioscience, **54**: 413-427.

Beschta RL. 1997. Riparian shade and stream temperature: an alternative perspective. Rangelands: 25-28.

Bogan T, Mohseni O, Stefan HG. 2003. Stream temperature-equilibrium temperature relationship. Wat. Res. Research, **39**: n/a-n/a. DOI: 10.1029/2003wr002034.

Brosofske KD, Chen J, Naiman RJ, Franklin J. 1997. Harvesting effects on microclimatic gradients from small streams ot uplands in western Washington. Ecol Appl, **7**: 1188-1200.

Brown LE, Hannah DM. 2008. Spatial heterogeneity of water temperature across an alpine river basin. Hydrological Processes, **22**: 954-967. DOI: 10.1002/hyp.6982.

Buisson L, Thuiller W, Lek S, Lim PUY, Grenouillet G. 2008. Climate change hastens the turnover of stream fish assemblages. Glob Change Biol, **14**: 2232-2248. DOI:

10.1111/j.1365-2486.2008.01657.x.

Burnham KP, Anderson DR. 2002. *Model Selection and Multimodel Inference: a Practical Information-Theoretic Approach, 2nd edition*. Springer.

Caissie D. 2006. The thermal regime of rivers: a review. Freshwater Biol, **51**: 1389-1406. DOI: 10.1111/j.1365-2427.2006.01597.x.

Constantz J. 1998. Interaction between stream temperature, streamflow, and groundwater exchanges in alpine streams. Wat. Res. Research, **34**: 1609-1615.

Crozier LG, Hendry AP, Lawson PW, Quinn TP, Mantua NJ, Battin J, Shaw RG, Huey RB. 2008. Potential responses to climate change in organisms with complex life histories: evolution and plasticity in Pacific salmon. Evolutionary Applications, **1**: 252-270. DOI: 10.1111/j.1752-4571.2008.00033.x.

Deitchman R, Loheide SPI. 2012. Sensitivity of thermal habitat of a trout stream to potential climate change, Wisconsin, United States. J Am Water Resour Assoc, **1**: 13. DOI: 10.1111/j.1752-1688.2012.00673.x.

Dent L, Vick D, Abraham K, Schoenholtz S, Johnson S. 2008. Summer temperature patterns in headwater streams of the Oregon Coast Range. J Am Water Resour Assoc, **44**: 803-813. DOI: 10.1111/j.1752-1688.2008.00204.x.

Dugdale SJ, Bergeron NE, St-Hilaire A. 2013. Temporal variability of thermal refuges and water temperature patterns in an Atlantic salmon river. Remote Sens Environ, **136**: 358-373. DOI: 10.1016/j.rse.2013.05.018.

Dugdale SJ, Bergeron NE, St-Hilaire, A. 2015. Spatial distribution of thermal refuges analyzed in relation to riverscape hydromorphology using airborne thermal infrared imagery. Remote Sensing of Environment, **160**: 43-55. DOI: 10.1016/j.rse.2014.12.021.

Ebersole JL, Liss WJ, Frissell CA. 1997. Restoration of stream habitats in the western United States: Restoration as reexpression of habitat capacity. Environmental Management **21**:1-14. DOI: 10.1007/s002679900001.

Ebersole JL, Wigington PJ Jr., Leibowitz SG, Comeleo RL, Van Sickle J. 2015. Predicting the occurrence of cold-water patches at intermittent and ephemeral tributary confluences with warm rivers. Freshwater Science, **34**: 111-124. DOI: 10.1086/678127.

Ficke AD, Myrick CA, Hansen LJ. 2007. Potential impacts of global climate change on freshwater fisheries. Rev Fish Biol Fish, **17**: 581-613. DOI: 10.1007/s11160-007-9059-5.

Glejser H. 1969. A new test for heteroskedasticity. Journal of the American Statistical Association, **64**: 315-323.

Hamlet AF. 2010. Assessing water resources adaptive capacity to climate change impacts in the Pacific Northwest Region of North America. Hydrology and Earth System Sciences Discussions, **7**: 4437-4471. DOI: 10.5194/hessd-7-4437-2010.

Handcock RN, Torgersen CE, Cherkauer KA, Gillespie AR, Tockner K, Faux RN, Tan J. 2012. Thermal infrared remote sensing of water temperature in riverine landscapes. In: *Fluvial Remote Sensing for Science and Management*, Carbonneau P, Piégay H (eds.) John Wiley & Sons, pp: 85-113.

Hanski I. 1998. Metapopulation dynamics. NATURE, **396**: 41-49. DOI: 10.1038/23876.

Harr RD. 1982. Fog drip in the Bull Run municipal watershed, Oregon. Water Resour Bull, **18**: 785-789.

Hill RA, Hawkins CP, Carlisle DM. 2013. Predicting thermal reference conditions for USA streams and rivers. Freshwater Science, **32**: 39-55. DOI: 10.1899/12-009.1.

ID DEQ (Idaho Department of Environmental Quality). 2000. Paired color infrared and thermal infrared imaging and analysis for selected Idaho streams. Prepared by IRZ Consulting, Hermiston, OR. http://www.deq.idaho.gov/media/528722-flir_2000.pdf

ID DEQ (Idaho Department of Environmental Quality). 2001. Paired color infrared and thermal infrared imaging and analysis for selected Idaho streams. Prepared by IRZ Consulting, Hermiston, OR. http://www.deq.idaho.gov/media/528718-flir_2001.pdf

IPCC, Scholes R, Settele J, Betts R, Bunn S, Leadley P, Nepstad D, Overpeck J, Taboada MA. 2014. Chapter 4. Terrestrial and inland water systems. *In* Climate Change 2014: Impacts, Adaptation and Vulnerability. Contribution of Working Group II to the Fifth Assessment Report of the Intergovernmental Panel on Climate Change. http://ipcc-wg2.gov/AR5/images/uploads/WGIIAR5-Chap4_FGDall.pdf. Cambridge University Press.

Isaak DJ, Peterson EE, Ver Hoef JM, Wenger SJ, Falke JA, Torgersen CE, Sowder C, Steel EA, Fortin M-J, Jordan CE, Ruesch AS, Som N, Monestiez P. 2014. Applications of spatial statistical network models to stream data. Wiley Interdisciplinary Reviews: Water. DOI: 10.1002/wat2.1023.

Isaak DJ, Wenger SJ, Peterson EE, Ver Hoef JM, Hostetler S, Luce CH, Dunham JB, Kershner J, Roper BB, Nagel D, Horan D, Chandler G, Parkes S, Wollrab S. 2013. NorWeST: An interagency stream temperature database and model for the Northwest United States. U.S. Fish and Wildlife Service, Great Northern Landscape Conservation Cooperative Grant. Project webpage: www.fs.fed.us/rm/boise/AWAE/projects/NorWeST.html (Aug 2014).

Isaak DJ, Wollrab S, Horan D, Chandler G. 2012. Climate change effects on stream and river temperatures across the northwest U.S. from 1980–2009 and implications for salmonid fishes. Clim Change, **113**: 499-524. DOI: 10.1007/s10584-011-0326-z.

Kaushal SS, Likens GE, Jaworski NA, Pace ML, Sides AM, Seekell D, Belt KT, Secor DH, Wingate RL. 2010. Rising stream and river temperatures in the United States. Front Ecol Environ, **8**: 461-466. DOI: 10.1890/090037.

Keery J, Binley A, Crook N, Smith JWN. 2007. Temporal and spatial variability of groundwater–surface water fluxes: Development and application of an analytical method using temperature time series. J Hydrol, **336**: 1-16. DOI: 10.1016/j.jhydrol.2006.12.003.

Kiffney PM, Greene CM, Hall JE, Davies JR. 2006. Tributary streams create spatial discontinuities in habitat, biological productivity, and diversity in mainstem rivers. Can J Fish Aquat Sci, **63**: 2518-2530. DOI: 10.1139/f06-138.

Legendre P. 1993. Spatial autocorrelation: trouble or new paradigm? Ecology, **74**: 1659-1673.

Luce C, Staab B, Kramer M, Wenger S, Isaak D, McConnell C. 2014. Sensitivity of summer stream temperatures to climate variability in the Pacific Northwest. Wat. Res. Research, **50**: 3428-3443. DOI: 10.1002/2013wr014329.

Madej MA, Currens C, Ozaki V, Yee J, Anderson DG. 2006. Assessing possible thermal rearing restrictions for juvenile coho salmon (*Oncorhynchus kisutch*) through thermal infrared imaging and in-stream monitoring, Redwood Creek, California. Can J Fish Aquat Sci, **63**: 1384-1396. DOI: 10.1139/f06-043.

Mantua N, Tohver I, Hamlet A. 2010. Climate change impacts on streamflow extremes and summertime stream temperature and their possible consequences for freshwater salmon habitat in Washington State. Clim Change, **102**: 187-223. DOI: 10.1007/s10584-010-9845-2.

Mayer TD. 2012. Controls of summer stream temperature in the Pacific Northwest. J Hydrol, **475**: 323-335. DOI: 10.1016/j.jhydrol.2012.10.012.

McKay L, Bondelid T, Dewald T, Rea A, Moore R. 2012. NHD Plus Verion 2: User Guide. Application-ready geospatial framework of U.S. surface-water data products associated with the USGS National Hydrography Dataset. URL www.horizon-systems.com/nhdplus/ (Jan 2014).

Monk WA, Wilbur NM, Curry RA, Gagnon R, Faux RN. 2013. Linking landscape variables to cold water refugia in rivers. J Environ Manage, **118**: 170-176. DOI: 10.1016/j.jenvman.2012.12.024.

Moore RD, Spittlehouse DL, Story A. 2005. Riparian microclimate and stream temperature response to forest harvesting: a review. J Am Water Resour Assoc, **04066**: 813-834.

Nash JE, Sutcliffe JV. 1970. River flow forecasting through conceptual models part I: a discussion of principles. J Hydrol, **10**: 282-290. DOI: 10.1016/0022-1694(70)90255-6.

Oregon Department of Environmental Quality, Umatilla Basin Watershed Council, The Confederated Tribes of the Umatilla Indian Reservation. 2001. Umatilla River Basin total maximum daily load (TMDL) and water quality management plan. Appendix A-4. Temperature Technical Analysis. pp: 74.

Peterson EE, Ver Hoef JM, Isaak DJ, Falke JA, Fortin MJ, Jordan CE, McNyset K, Monestiez P, Ruesch AS, Sengupta A, Som N, Steel EA, Theobald DM, Torgersen CE, Wenger SJ. 2013. Modelling dendritic ecological networks in space: an integrated network perspective. Ecol Lett. DOI: 10.1111/ele.12084.

Pinheiro J, Bates D, DebRoy S, Sarkar D, R Development Core Team. 2012. nlme: Linear and Nonlinear Mixed Effects Models. R package version 3.1-105.

Pinheiro JC, Bates DM. 2000. *Mixed-Effects Models in S and S-PLUS*. Springer-Verlag.

Poole GC. 2002. Fluvial landscape ecology: addressing uniqueness within the river discontinuum. Freshwater Biol, **47**: 641-660. DOI: 10.1046/j.1365-2427.2002.00922.x.

Poole GC, Berman CH. 2001. An ecological perspective on in-stream temperature: natural heat dynamics and mechanisms of human-caused thermal degradation. Environ Manage, **27**: 787-802. DOI: 10.1007/s002670010188.

R Development Core Team. 2012. R: A language and environment for statistical computing. R Foundation for Statistical Computing, Vienna, Austria. ISBN 3-900051-07-0, URL www.R-project.org/.

Rice SP, Greenwood MT, Joyce CB. 2001. Tributaries, sediment sources, and the longitudinal organisation of macroinvertebrate fauna along river systems. Can J Fish Aquat Sci, **58**: 824-840. DOI: 10.1139/cjfas-58-4-824.

Schindler DE, Hilborn R, Chasco B, Boatright CP, Quinn TP, Rogers LA, Webster MS. 2010. Population diversity and the portfolio effect in an exploited species. Nature, **465**: 609-612. DOI: 10.1038/nature09060.

Schlosser IJ. 1995. Critical landscape attributes that influence fish population-dynamics in headwater streams. Hydrobiologia, **303**: 71-81. DOI: 10.1007/978-94-017-3360-1_7.

Stanford JA, Ward JV. 2001. Revisiting the serial discontinuity concept. Regul Rivers Res Manage, **17**: 303-310. DOI: 10.1002/rrr.659.

Steel EA, Lange IA. 2007. Using wavelet analysis to detect changes in water temperature regimes at multiple scales: effects of multi-purpose dams in the Willamette River basin. River Res Appl, **23**: 351-359. DOI: 10.1002/rra.985.

Steel EA, Tillotson A, Larsen DA, Fullerton AH, Denton KP, Beckman BR. 2012. Beyond the mean: The role of variability in predicting ecological effects of stream temperature on salmon. Ecosphere, **3**: art104. DOI: 10.1890/es12-00255.1.

Tague C, Farrell M, Grant G, Lewis S, Rey S. 2007. Hydrogeologic controls on summer stream temperatures in the McKenzie River basin, Oregon. Hydrological Processes, **21**: 3288-3300.

Tague C, Grant G, Farrell M, Choate J, Jefferson A. 2008. Deep groundwater mediates streamflow response to climate warming in the Oregon Cascades. Clim Change, **86**: 189-210. DOI: 10.1007/s10584-007-9294-8.

Theurer FD, Lines I, Nelson T. 1985. Interaction between riparian vegetation, water temperature, and salmonid habitat in the Tucannon River. Water Resour Bull, **21**: 53-64. DOI: 10.1111/j.1752-1688.1985.tb05351.x.

Tonolla D, Acuña V, Uehlinger U, Frank T, Tockner K. 2010. Thermal heterogeneity in river floodplains. Ecosystems, **13**: 727-740. DOI: 10.1007/s10021-010-9350-5.

Torgersen CE, Faux RN, McIntosh BA. 1999. Aerial survey of the Upper McKenzie River: Thermal infrared and color videography. Oregon State University.

Torgersen CE, Faux RN, McIntosh BA, Poage NJ, Norton DJ. 2001. Airborne thermal remote sensing for water temperature assessment in rivers and streams. Remote Sens Environ, **76**: 386-398. DOI: 10.1016/S0034-4257(01)00186-9.

Torgersen CE, Price DM, Li HW, McIntosh BA. 1999. Multiscale thermal refugia and stream habitat associations of chinook salmon in northeastern Oregon. Ecol Appl, **9**: 301-319.

van Vliet MTH, Ludwig F, Kabat P. 2013. Global streamflow and thermal habitats of freshwater fishes under climate change. Clim Change, **121**: 739-754. DOI: 10.1007/s10584-013-0976-0.

van Vliet MTH, Ludwig F, Zwolsman JJG, Weedon GP, Kabat P. 2011. Global river temperatures and sensitivity to atmospheric warming and changes in river flow. Wat. Res. Research, **47**. DOI: 10.1029/2010wr009198.

Vannote RL, Minshall GW, Cummins KW, Sedell JR, Cushing CE. 1980. River Continuum Concept. Can J Fish Aquat Sci, **37**: 130-137.

Ward JV. 1985. Thermal characteristics of running waters. Hydrobiologia, **125**: 31-46. DOI: 10.1007/978-94-009-5522-6_3.

Ward JV, Stanford JA. 1983. The serial discontinuity concept of lotic ecosystems. In: *Dynamics of lotic ecosystems*, Fontaine TD, Bartell SM (eds.) Ann Arbor Science Publishers, pp: 29-42.

Webb BW, Hannah DM, Moore RD, Brown LE, Nobilis F. 2008. Recent advances in stream and river temperature research. Hydrological Processes, **22**: 902-918. DOI: 10.1002/hyp.

Webb BW, Nobilis F. 1995. Long term water temperature trends in Austrian rivers. Hydrological Sciences, **40**: 83-95. DOI: 10.1080/02626669509491392.

Welty, EZ. 2015. Linbin: Binning and plotting of linearly referenced data. R package version 0.1.0. https://github.com/ezwelty/linbin; http://cran.r-project.org/web/packages/linbin/index.html. [Forthcoming: Welty EZ, Torgersen CE, Brenkman SJ, Duda JJ, Armstrong JB. In Review. Multiscale longitudinal analysis of river networks using the *linbin* R package. N Am J Fish Manage.]

Wu H, Kimball JS, Elsner MM, Mantua N, Adler RF, Stanford J. 2012. Projected climate change impacts on the hydrology and temperature of Pacific Northwest rivers. Wat. Res. Research, **48**. DOI: 10.1029/2012wr012082.

Table 1. Attributes of remotely sensed profiles of summertime river temperature used in analyses

Basin/River (Map Reference)	First day of survey	Total length surveyed (km)	Flight duration (h)	Proportion of river surveyed	Strahler stream orders (n)	Distance-weighted mean Strahler order [5]	Survey midpoint (km from mouth / total km)	TIR Accuracy (mean ± sd, °C) [6]	Discharge in survey year (percentile) [7]	Profile class (second choice)
Bear										
Cub (1)	29 Jul 06	56	1.11	0.94	2	3.6	0.47	0.1±0.08	0.50	A (C)
Deschutes										
Crooked[1] (2)	6 Aug 2005[2]	224	2.63	0.88	3	6.0	0.45	0.47±0.36	0.32	C (P)
Little Deschutes (3)	24 Jul 2001	144	1.80 [3]	1.00	4	3.5	0.50	0.43±0.05	NA	A
Whychus (4)	28 Jul 2000	58	0.90	0.75	4	3.0	0.62	0.36±0.21	NA	C (L)
John Day										
John Day[1] (5)	29 Aug 2004[2]	446	6.42 [3,4]	1.00	5	5.5	0.50	0.32±0.2	0.54	A (L)
Middle Fork John Day (6)	5 Aug 1998	74	0.76	0.59	2	4.5	0.62	0.35±0.51	0.88	L (C)
Middle Fork John Day (7)	16 Aug 2003	76	1.16	0.64	2	4.5	0.61	0.48±0.12	0.57	L (C)
North Fork John Day (8)	11 Aug 2002	139	2.42 [3]	0.79	2	5.6	0.40	0.62±0.57	0.26	A (L)
South Fork John Day (9)	15 Aug 2003	83	1.41	0.67	3	3.8	0.66	0.38±0.15	NA	C (L)
Klamath										
Scott[1] (10)	25 Jul 2003	116	1.64	1.00	4	4.2	0.50	0.31±0.22	0.65	C (L)
Scott (11)	10 Aug 2006	92	1.28	0.80	2	4.6	0.40	0.11±0.11	0.46	U (C)
Shasta (12)	26 Jul 2003	65	1.19	0.74	3	4.4	0.37	0.4±0.32	0.80	L
Sprague[1] (13)	12 Aug 1999	169	1.50	0.97	4	5.3	0.48	0.49±0.31	0.50	A
Sprague[1] (14)	31 Jul 2007[2]	172	2.78 [4]	0.94	4	5.4	0.47	0.34±0.39	0.11	A (C)
Williamson (15)	4 Aug 1999	139	1.08	1.00	4	4.4	0.50	0.62±0.36	0.62	C (U)
Lower Columbia										
Sandy (16)	8 Aug 2001	86	1.21	1.00	4	4.3	0.50	0.38±0.26	0.26	A (C)
Lower Snake										
Clearwater[1] (17)	3 Aug 2000	151	1.47 [3]	0.57	2	5.4	0.54	2.65±3.04	0.45	L (C)
Grande Ronde[1] (18)	19 Aug 1999[2]	273	2.43	0.98	4	5.6	0.49	0.48±0.19	NA	C (L)

Basin/River (Map Reference)	First day of survey	Total length surveyed (km)	Flight duration (h)	Proportion of river surveyed	Strahler stream orders (n)	Distance-weighted mean Strahler order [5]	Survey midpoint (km from mouth / total km)	TIR Accuracy (mean ± sd, °C) [6]	Discharge in survey year (percentile) [7]	Profile class (second choice)
Joseph[1] (19)	22 Aug 1999	118	1.07	0.96	5	4.3	0.52	0.4±0.35	NA	C (A)
Lochsa[1] (20)	4 Aug 2000[2]	153	1.20	0.80	2	5.4	0.40	1.15±0.83	0.16	L
Minam (21)	21 Aug 1999	73	0.59	0.85	4	3.5	0.57	0.75±0.78	0.77	L
Salmon[1] (22)	8 Aug 2001[2]	645	5.74 [3,4]	0.96	3	6.3	0.48	0.5±	0.02	A (C)
Selway[1] (23)	4 Aug 2000[2]	153	1.58 [3]	0.75	2	5.6	0.37	1.4±0.6	0.15	A (L)
Wallowa (24)	23 Aug 1999	80	0.81	0.78	3	3.9	0.39	0.43±0.5	0.84	L (C)
Middle Columbia										
Eightmile (25)	3 Aug 2002	54	1.38	0.92	3	2.5	0.54	0.58±0.34	NA	P (A)
Fifteenmile (26)	1 Aug 2002	83	1.64	1.00	4	3.6	0.50	0.49±0.26	NA	P (A)
Touchet[1] (27)	8 Aug 2002[2]	119	2.08	0.82	5	5.1	0.51	0.29±0.13	NA	A
Walla Walla[1] (28)	15 Aug 2000	109	2.20	0.92	5	5.0	0.46	0.4±0.42	0.47	P (A)
Walla Walla[1] (29)	13 Aug 2003	97	1.76	0.85	5	5.2	0.43	0.39±0.17	0.44	P (A)
N California Coastal										
Eel[1] (30)	11 Aug 2005[2]	186	2.33 [3,4]	0.60	2	7.0	0.33	0.32±0.29	0.78	P
Mattole (31)	19 Jul 2001	111	1.67	0.97	3	3.7	0.51	0.4±0.3	0.28	P
Redwood (32)	29 Jul 2003	95	1.60 [3]	0.93	3	3.5	0.47	0.35±0.21	0.38	P
Russian[1] (33)	23 Jul 2004[2]	157	2.69 [3,4]	0.79	2	5.0	0.45	0.32±0.25	0.54	A
N Oregon Coastal										
Nehalem (34)	5 Aug 2000	179	3.04	0.91	4	4.1	0.49	0.36±0.28	0.29	P (C)
Siletz[1] (35)	5 Aug 2001	103	1.54	0.84	4	4.4	0.58	0.2±0.14	0.74	A
Puget Sound										
Deschutes (36)	19 Aug 2003	68	1.16	0.83	2	3.0	0.44	0.14±0.09	0.02	U (P)
Nooksack[1] (37)	20 Aug 2001	120	1.46	1.00	4	3.9	0.50	0.64±0.6	0.67	C (A)
Snoqualmie[1] (38)	13 Aug 2006	103	3.47 [3,4]	0.79	2	4.6	0.39	0.08±0.04	0.23	L (C)
NF Stillaguamish[1] (39)	7 Sep 2001	93	1.65 [4]	0.89	4	3.6	0.45	0.23±0.21	0.81	A

Basin/River (Map Reference)	First day of survey	Total length surveyed (km)	Flight duration (h)	Proportion of river surveyed	Strahler stream orders (n)	Distance-weighted mean Strahler order [5]	Survey midpoint (km from mouth / total km)	TIR Accuracy (mean ± sd, °C) [6]	Discharge in survey year (percentile) [7]	Profile class (second choice)
SF Stillaguamish[1] (40)	8 Sep 2001	100	1.45	0.93	3	3.4	0.47	0.17±0.15	NA	A (L)
S Oregon Coastal										
Applegate (41)	18 Aug 1998	75	0.64	0.78	2	4.8	0.39	0.24±0.12	0.94	A (L)
Applegate (42)	19 Jul 1999	75	0.66	0.79	2	4.7	0.39	0.15±0.14	0.96	A
Cow (43)	25 Jul 2000	96	1.31	0.51	2	4.0	0.61	0.54±0.48	0.86	A
Evans[1] (44)	1 Aug 2003	56	0.98	0.69	3	3.5	0.65	0.46±0.21	NA	A
Little Butte[1] (45)	13 Jul 2001	62	1.05	0.94	3	3.3	0.47	0.26±0.26	NA	C (A)
North Umpqua (46)	25 Jul 2002	85	1.33 [3]	0.71	3	4.7	0.36	0.33±0.31	0.14	L
Rogue[1] (47)	30 Jul 2003[2]	261	2.62	0.72	2	5.6	0.37	0.32±0.25	0.45	A
Umpqua[1] (48)	23 Jul 2002[2]	289	5.16 [3]	0.81	5	5.4	0.50	0.47±0.42	0.10	A
Upper Columbia										
Entiat (49)	11 Aug 2001	78	1.95	0.98	7	3.9	0.49	0.17±0.06	NA	A
Wenatchee[1] (50)	13 Aug 2001[2]	89	1.15	0.70	4	4.4	0.65	0.2±0.16	0.12	A (P)
Washington Coastal										
Hoh (51)	25 Sep 2000	60	0.70	0.67	2	3.8	0.34	0.5±0.31	0.67	A (L)
Willapa (52)	30 Aug 2001	61	1.56	0.85	4	3.8	0.55	0.83±0.32	1.00	A
Willamette										
Molalla (53)	26 Jul 2004	76	1.44 [3]	0.99	5	4.0	0.49	0.4±0.2	0.26	A
Pudding[1] (54)	11 Aug 2004[2]	107	2.97 [3,4]	0.97	4	4.5	0.52	0.08±0.08	0.72	U
Thomas (55)	3 Aug 2000	50	0.87	0.81	3	3.5	0.47	0.33±0.15	NA	A (L)
Tualatin[1] (56)	27 Jul 1999	129	1.38 [4]	1.00	4	4.2	0.50	0.36±0.27	0.90	C (L)
Yamhill (57)	27 Jul 2005	103	1.93	0.90	3	5.0	0.45	0.38±0.29	0.83	A
Yakima										

Basin/River (Map Reference)	First day of survey	Total length surveyed (km)	Flight duration (h)	Proportion of river surveyed	Strahler stream orders (n)	Distance-weighted mean Strahler order [5]	Survey midpoint (km from mouth / total km)	TIR Accuracy (mean ± sd, °C) [6]	Discharge in survey year (percentile) [7]	Profile class (second choice)
Naches (58)	14 Aug 2004	72	1.28 [3]	0.76	3	5.3	0.38	0.27±0.21	NA	U (C)
MEAN		**127**	**1.41**	**0.85**	**3.3**	**4.5**	**0.48**	**0.44**	**0.51**	
SD		**98**	**0.58**	**0.13**	**1.1**	**0.9**	**0.08**	**0.37**	**0.29**	

[1] Adjacent surveys were combined; [2] Survey was conducted over 2 days; [3] Survey occurred in a downstream direction; [4] Upstream section of a combined survey was surveyed first

[5] Weighted average stream order, calculated as $\sum_n^1(S_j * L_j)/\sum_n^1 L_j$ where S_j = Strahler stream order in reach j, L_j = length (km) of reach j, and n = all reaches in the survey (reach data from NHDPlusV2 hydrography dataset [*McKay et al.* 2012])

[6] Absolute deviation between radiant temperature (from TIR) and instream temperature measured with Onset loggers at a variety of locations throughout the river (source: project completion reports, available on request)

[7] Percentile of discharge in survey year relative to period of record for gages located on, upstream of, or downstream of thermal infrared surveys (mean of 2 gages per survey; range 1-6) and for the month in which the TIR survey was conducted. NA: Data were not available for all surveys. Source: USGS (http://waterdata.usgs.gov/nwis). We computed statistics only when a complete monthly record was available.

Table 2. Rivers with a large dam (≥15 m tall) near the reach surveyed

Profile	Dam name[1]	Height (m)	Position of dam relative to survey	Profile class	Predicted shape if dam were absent
Applegate 1998, 1999	Applegate	73.8	Upstream end	asymptotic	Remain asymptotic, possibly linear
Cow 2000	Galesville	50.9	Upstream end	asymptotic	Remain asymptotic, possibly linear
Crooked 2005	Arthur R. Bowman	74.7	Middle, near Prineville	complex	Complex regardless due to other factors
Rogue 2003	William L. Jess	105.2	Upstream end	asymptotic	Remain asymptotic
Russian 2004	Coyote Valley	54.9	Upstream end	asymptotic	Remain asymptotic, possibly linear
Shasta 2003	Shasta River	29.3	Upstream end	linear	Remain linear, possibly asymptotic
Tualatin 1999	Scoggins	151.0	In Scoggins Creek (tributary in middle of profile)	complex	Asymptotic or linear

[1] Source: 2013 National Inventory of Dams dataset (http://nid.usace.army.mil)

Table 3. Summary characteristics of surveys in each thermal profile class

	Survey		Median (95% confidence interval)				
Profile class	(n)	No. less certain (n)[1]	Profile length (km)	Proportion of river surveyed	Midpoint of profile in river	Strahler orders (n)	Weighted average Strahler order[2]
Asymptotic	27	12	100	0.83	0.48	3.0	4.7
			(54-516)	(0.61-1.0)	(0.36-0.65)	(2.0-5.7)	(3.4-6.1)
Linear	9	5	80	0.74	0.40	2.0	4.5
			(67-153)	(0.58-0.84)	(0.36-0.62)	(2.0-3.8)	(3.6-5.4)
Parabolic							
Inland	4	2	90	0.92	0.48	4.5	4.3
			(56-108)	(0.86-0.99)	(0.43-0.53)	(3.1-5.0)	(2.6-5.2)
Coastal	4	1	152	0.92	0.48	3.0	3.9
			(96-185)	(0.62-0.97)	(0.34-0.51)	(2.1-3.9)	(3.5-6.8)
Uniform	4	3	82	0.81	0.42	2.5	4.5
			(68-106)	(0.77-0.96)	(0.38-0.51)	(2.0-3.9)	(3.1-5.2)
Complex	10	0	119	0.97	0.50	4	4.2
			(58-262)	(0.70-1.0)	(0.46-0.65)	(3.0-4.8)	(3.4-5.6)

[1] Surveys for which classification was less certain based on goodness of fit diagnostics
[2] See footnote 5 in Table 1

Table 4. Mean of partial correlation coefficients describing relationships between river temperature and hydroclimatic variables for each thermal profile class

Profile class	Elevation	Mean August air temperature	Mean August precip-itation	Discharge	Velocity	Gradient	Tributary temperature	Distance upstream
Asymptotic	-0.49	0.37	-0.29	0.00	0.14	-0.27	0.50	-0.78
Linear	0.02	-0.03	-0.11	-0.08	0.00	-0.03	0.13	-0.83
Parabolic								
Inland	-0.83	0.82	-0.60	-0.33	0.25	-0.47	0.78	-0.85
Coastal	-0.53	0.78	-0.09	-0.69	-0.04	-0.23	0.25	0.01
Uniform	-0.10	-0.07	0.10	-0.13	-0.22	-0.42	0.58	0.17
Complex	-0.21	0.10	-0.05	-0.11	-0.08	-0.24	0.69	-0.27

Table 5. Median (95% confidence interval) of network metrics for each profile class

Profile class	Basin shape	Stream density	Significant confluence density
Asymptotic	0.12 (0.04-0.23)	0.69 (0.44-0.86)	0.04 (0.02-0.12)
Linear	0.21 (0.08-0.31)	0.70 (0.43-0.80)	0.05 (0.03-0.08)
Parabolic			
Inland	0.22 (0.10-0.35)	0.82 (0.74-1.01)	0.07 (0.04-0.08)
Coastal	0.07 (0.06-0.09)	0.79 (0.68-0.89)	0.09 (0.02-0.12)
Uniform	0.16 (0.07-0.27)	0.71 (0.59-0.77)	0.08 (0.05-0.09)
Complex	0.13 (0.09-0.33)	0.63 (0.31-0.77)	0.07 (0.02-0.11)

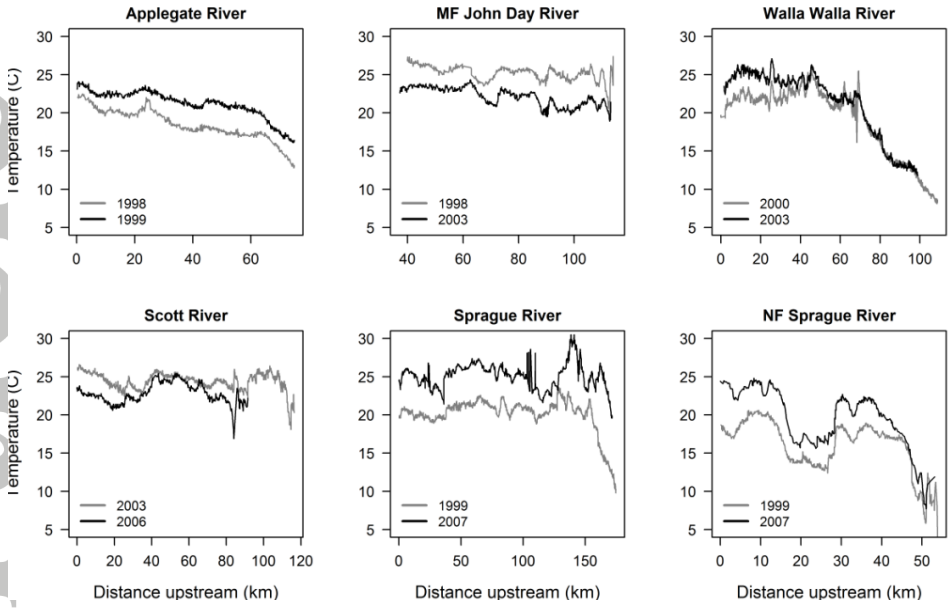

Figure 1. Longitudinal profiles for rivers in which surveys were flown in two years, illustrating similar spatial variance patterns. The NF Sprague River did not meet analysis criteria, but we included it here to illustrate consistency among years.

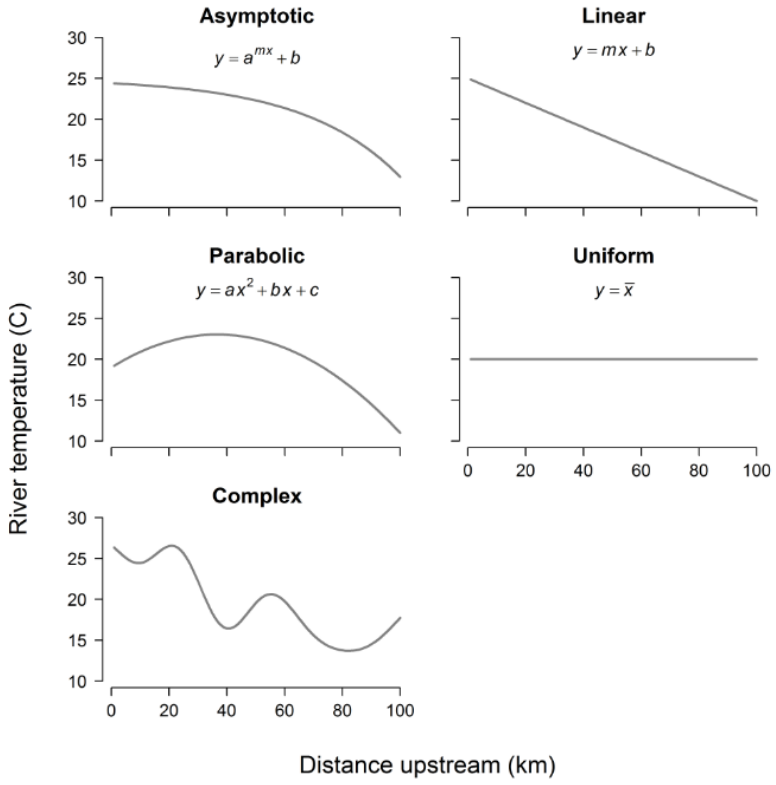

Figure 2. Theoretical representations and model equations for the five thermal profile classes, where ***y*** is river temperature (°C), ***x*** is the distance upstream from the downstream terminus of the profile (km), and a, b, c, and m are constants.

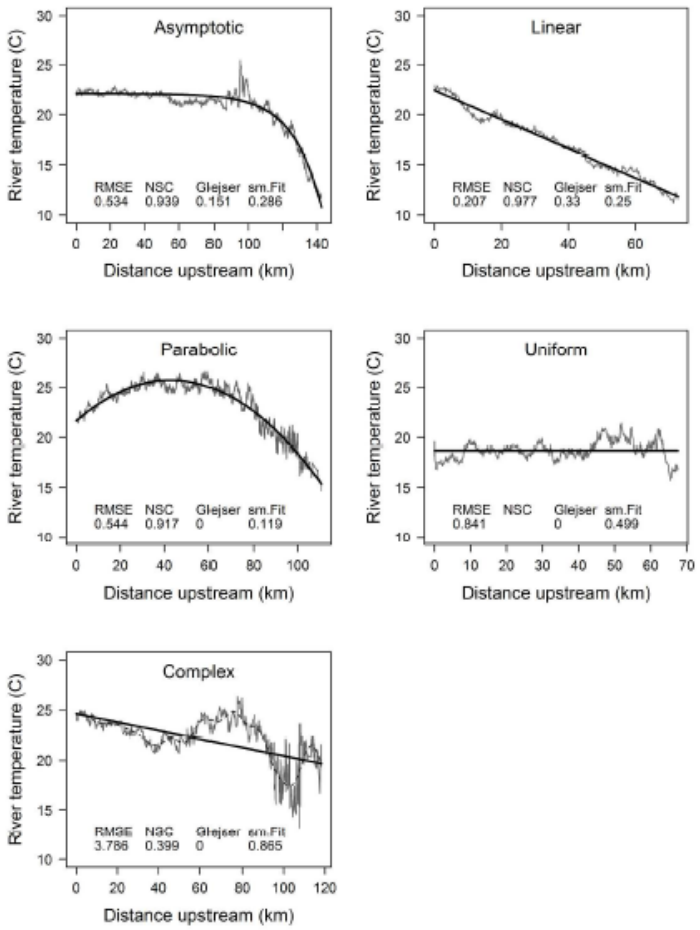

Figure 3. Examples of profile classification and diagnostics for *asymptotic*, *linear*, *parabolic*, *uniform*, and *complex* profiles. For each example, the plot shows river temperature vs. distance surveyed in gray and fitted values for the best model selected from the candidate set in black. Diagnostic goodness of fit metrics root mean square error (RMSE), Nash-Sutcliffe Coefficient (NSC), p-value from a Glejser test for homoscedasticity (Glejser), and the difference in RMSE between the best model and a smoothed trend (20-knot GAM; sm.Fit) are shown on each plot. For the *complex* profile example, diagnostic values refer to the *linear* fit (solid line); the smoothed fit (dotted line) is also presented to illustrate the trend. The rivers shown are Asymptotic: Little Deschutes River (2001); Linear: Minam River (1999); Parabolic: Mattole River (2001); Uniform: Deschutes River (Puget Sound) (2003); and Complex: Joseph Creek (1999). Plots of other profiles are provided in Figure A2.

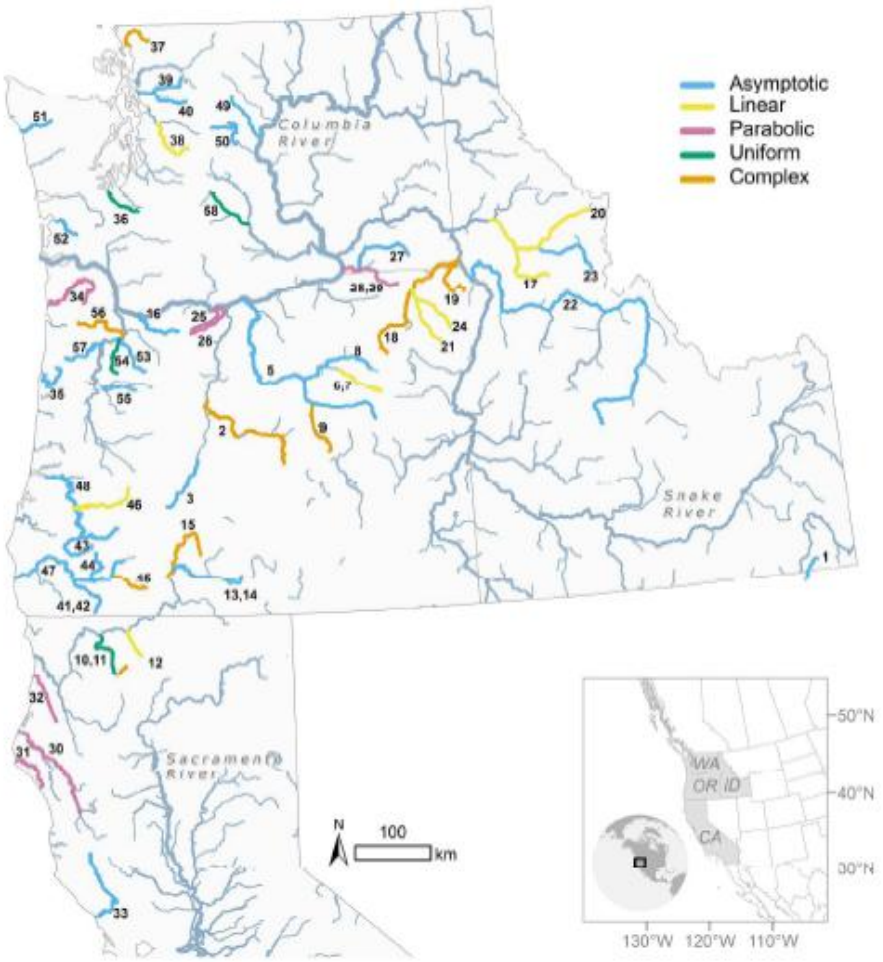

Figure 4. Geographic locations of rivers in each profile class.

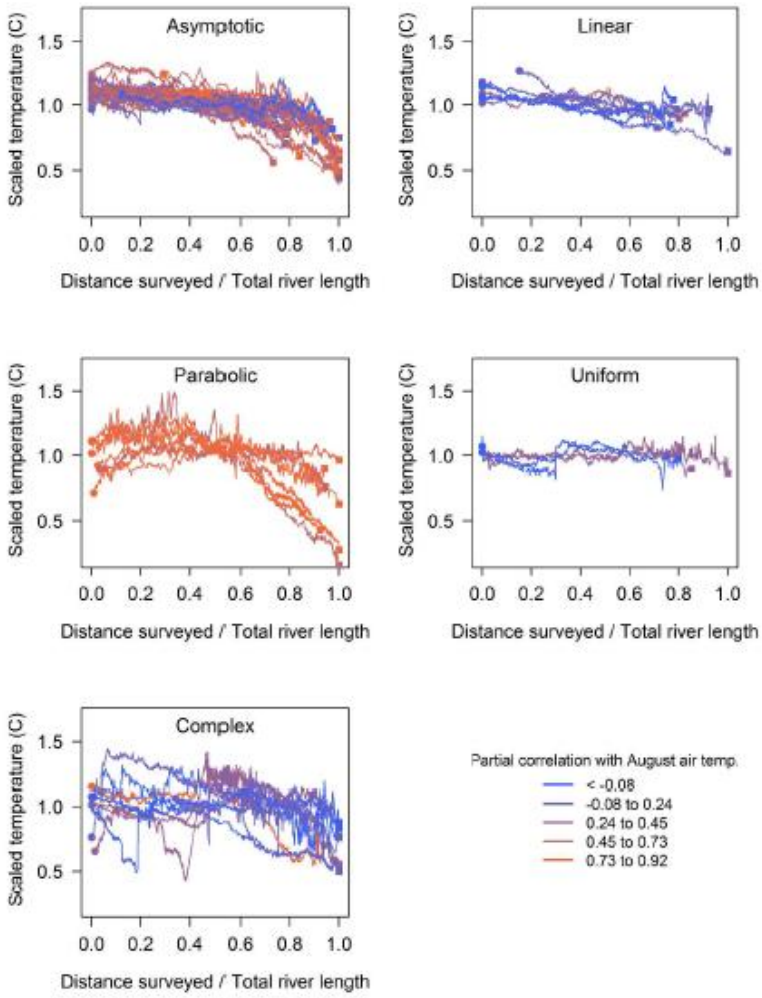

Figure 5. Partial correlations between river temperature and mean August air temperature for longitudinal profiles assigned to each class (*asymptotic*, *linear*, *parabolic*, *uniform*, and *complex*). The longitudinal profiles within each class are standardized on both axes to facilitate comparison of partial correlations among profiles. The downstream (circles) and upstream (squares) end points of individual surveys are demarcated to indicate the extent of the river included in each survey. Non-standardized plots of longitudinal profiles for all rivers assigned to each profile class are provided in Figure A2.

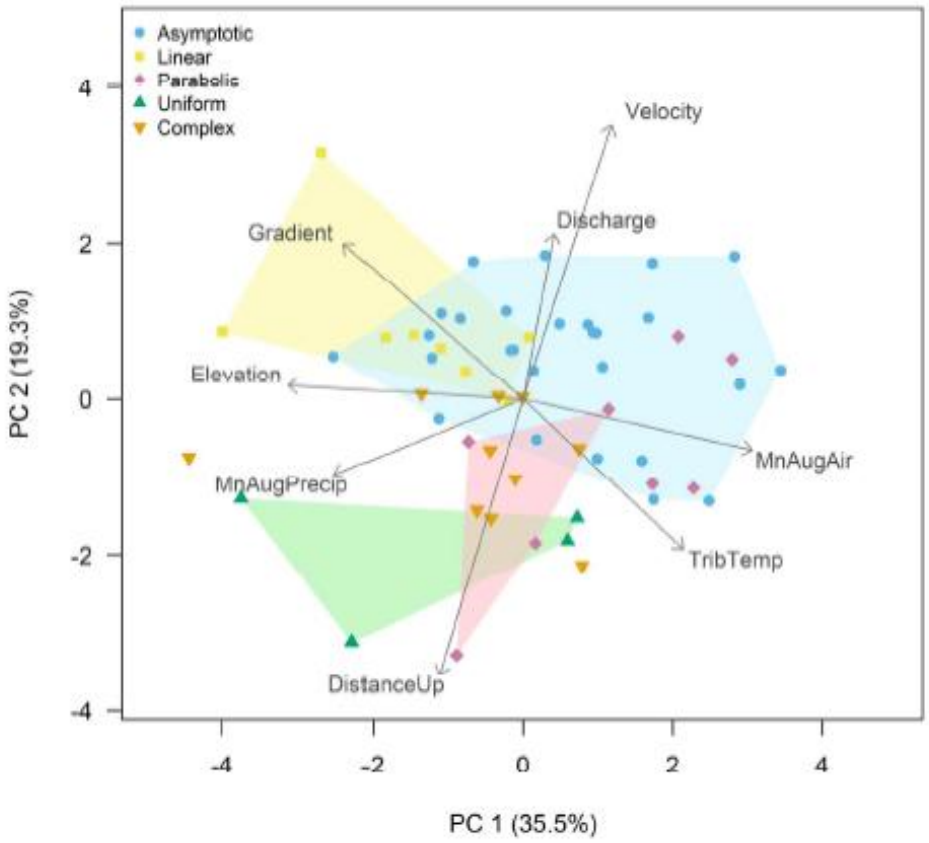

Figure 6. Principal components analysis (PCA) biplot showing the relationship in multivariate space of river temperature profiles (symbols) with respect to the strength and direction of partial correlations between water temperature and hydroclimatic variables (arrows). Note that the ordination is of partial correlation coefficients. Symbols indicate the class to which each profile was assigned. Colored polygons enclose symbols of the same color, with blue for *asymptotic*, yellow for *linear*, green for *uniform*, and pink for coastal *parabolic* profiles. Inland *parabolic* profiles are pink symbols within the blue polygon. Abbreviations: MnAugAir, mean August air temperature; MnAugPpt, mean August precipitation; TribTemp, temperature of tributaries; and DistanceUp, distance upstream.